

8937
Stinesifer

NRL Report 7020

Prediction of the Strengths of Internal Cavities in Glass Under Compressive Loads

J. A. KIES, R. J. SANFORD, AND D. R. MULVILLE

*Ocean Materials Criteria Branch
Ocean Technology Division*

January 30, 1970



NAVAL RESEARCH LABORATORY
Washington, D.C.

This document has been approved for public release and sale; its distribution is unlimited.

DOCUMENT CONTROL DATA - R & D

(Security classification of title, body of abstract and indexing annotation must be entered when the overall report is classified)

1. ORIGINATING ACTIVITY (Corporate author) Naval Research Laboratory Washington, D.C. 20390		2a. REPORT SECURITY CLASSIFICATION Unclassified	
		2b. GROUP	
3. REPORT TITLE PREDICTION OF THE STRENGTHS OF INTERNAL CAVITIES IN GLASS UNDER COMPRESSIVE LOADS			
4. DESCRIPTIVE NOTES (Type of report and inclusive dates) An interim report on one phase of the problems.			
5. AUTHOR(S) (First name, middle initial, last name) Joseph A. Kies, Robert J. Sanford, and Daniel R. Mulville			
6. REPORT DATE January 30, 1970		7a. TOTAL NO. OF PAGES 22	7b. NO. OF REFS 9
6a. CONTRACT OR GRANT NO. F01-05 and F01-03		9a. ORIGINATOR'S REPORT NUMBER(S) NRL Report 7020	
b. PROJECT NO. A32-520/652/69-R007-02-01			
c. RR 009-03-45-5450		9b. OTHER REPORT NO(S) (Any other numbers that may be assigned this report)	
d.			
10. DISTRIBUTION STATEMENT This document has been approved for public release and sale; its distribution is unlimited.			
11. SUPPLEMENTARY NOTES		12. SPONSORING MILITARY ACTIVITY Department of the Navy (Naval Air Systems Command and Office of Naval Research), Washington, D.C. 20360	
13. ABSTRACT The compressive strength of bulk glass is limited by the tensile strength of the surfaces of internal cavities, especially clusters of cavities closely spaced so as to have strongly interacting stress fields. The tensile stress on the surfaces of single ellipsoids were taken from a previous report, and predictions of probabilities of failure were made based on an assumed Weibull distribution of strengths. Numerical values for Weibull coefficients were used which were believed to be representative of pristine glass but <u>not</u> homogenized by extended heat treatment. The predictions are thought to be somewhat conservative but could easily be adjusted in the light of better experimental data if and when they become available. The assumed m coefficients are believed to be realistic but the assumed σ_0 , i.e., the strength of pristine bubbles of unit area at a probability of failure of 0.63, may need future revision. All predicted strengths are proportional to σ_0 . Predicted strengths are shown graphically for probabilities of failure ranging from 10^{-8} to 10^{-1} .			

14. KEY WORDS	LINK A		LINK B		LINK C	
	ROLE	WT	ROLE	WT	ROLE	WT
Compressive strength Strength of glass Ellipsoidal cavities Weibull distribution Size effect on bubble strength Needle-shaped cavities Prolate ellipsoids Spherical shells Cylindrical shells Membrane stress						

CONTENTS

Abstract	ii
Problem Status	ii
Authorization	ii
INTRODUCTION	1
STATISTICAL CONSIDERATIONS	1
THE SIZE EFFECT	4
EFFECTIVE AREAS OF ELLIPSOIDAL CAVITIES UNDER COMPRESSIVE LOADING – SPECIAL CASES	5
Uniaxial Compression, Spherical Cavity	5
Needle-Shaped Cavity, Parallel with Shell Axis, in a Cylindrical Shell Under Hydrostatic Pressure	5
Needle-Shaped Cavity Parallel with a Spherical Shell Wall Under Hydrostatic Pressure	9
Spherical Cavity in a Spherical Shell Under Hydrostatic Pressure	10
PREDICTED FRACTURE STRENGTH OF INTERNAL CAVITIES	10
Spherical Cavity Under Applied Uniaxial Compressive Stress	11
Needle-Shaped Cavity in a Cylindrical Shell Under Hydrostatic Compression	12
Needle-Shaped Cavity in a Spherical Shell	14
Spherical Cavity in a Spherical Shell	15
CONCLUSIONS	15
REFERENCES	18

ABSTRACT

The compressive strength of bulk glass is limited by the tensile strength of the surfaces of internal cavities, especially clusters of cavities closely spaced so as to have strongly interacting stress fields. The tensile stress on the surfaces of single ellipsoids were taken from a previous report, and predictions of probabilities of failure were made based on an assumed Weibull distribution of strengths. Numerical values for Weibull coefficients were used which were believed to be representative of pristine glass but not homogenized by extended heat treatment. The predictions are thought to be somewhat conservative but could easily be adjusted in the light of better experimental data if and when they become available. The assumed m coefficients are believed to be realistic but the assumed σ_0 , i.e., the strength of pristine bubbles of unit area at a probability of failure of 0.63, may need future revision. All predicted strengths are proportional to σ_0 . Predicted strengths are shown graphically for probabilities of failure ranging from 10^{-6} to 10^{-1} .

PROBLEM STATUS

This is an interim report on continuing NRL problems, under the sponsorship of the Naval Air Systems Command, entitled "Nonmetallic Materials, Fracture Strength." Mr. Charles F. Bersch, Code 52032A, is the sponsor's program manager. The work being reported on was also partly supported by the Office of Naval Research on a program entitled, "Fracture Strength."

AUTHORIZATION

NRL Problem F01-05
Project A32-520/652/69-R007-02-01
NRL Problem F01-03
Project RR 009-03-45-5450

Manuscript submitted November 5, 1969.

PREDICTION OF THE STRENGTHS OF INTERNAL CAVITIES IN GLASS UNDER COMPRESSIVE LOADS

INTRODUCTION

Bulk glass is now in widespread use for flotation spheres and for microballoons in syntactic foam. Manned capsules for deep submergence are in development but require a very high degree of reliability and high compressive strength. The case for glass pressure hulls and plans for their development have been set forth in considerable detail by H. Perry (1). A considerable amount of effort has been expended on the fabrication of large glass hemispheres (2).

Bubbles are difficult to eliminate entirely in bulk glass, and their surfaces experience tensile stresses nonuniformly distributed when the shell is under hydrostatic compression. Maximum values for tensile stresses on the surfaces of various ellipsoidal cavities in typical compressive loading situations were described in Ref. 3. The breaking strength of the bubbles is expected to depend on size, although the stress does not. The bubble strength is expected to be higher than the tensile strength of external surfaces of test specimens such as those in the concentric-ring test. The reasons are closely related; first, the surface of the cavity should have much less severe flaws, and, second, the size effect on strength is in favor of small bubbles. The effects of size and of surface quality are examined here in order to predict which single bubbles should be rejected as unsafe and which should be acceptable for an arbitrarily selected risk of failure.

Although the internal surfaces of bubbles are not subject to scratches or impact damage, there are always local variations in composition including seeds or crystalline particles which may introduce scatter in the tensile strength of the material. Statistics for bubble strengths are apparently not available; however, statistics for pristine fibers in liquid nitrogen are available although not yet published. Carefully homogenized E-glass fibers tested in liquid nitrogen exhibit a coefficient of variation of 8.7 percent, corresponding to a Weibull m coefficient of 14.* Glass fibers of the same composition but not homogenized exhibit a coefficient of variation of 15.9 percent, corresponding to $m = 7.5$. The extent to which moisture may increase the scatter or decrease m is not discussed in this report, although it is conceivable but not proved whether or not water dissolved in glass can affect fracture behavior. It is to be expected, on the basis of the foregoing, that the strengths of internal cavities in glass will exhibit a size effect. The strength is a function of the probability of failure. The numerical predicted strengths of single bubbles in this report are thought to be somewhat conservative, but for clusters of bubbles with stress fields interacting, the strengths would be much less.

STATISTICAL CONSIDERATIONS

Figure 1 shows the probability of failure in glass lantern slides vs applied stress at two different crosshead speeds. It is obvious that strength is a function of the probability of failure and of the testing speed. The effects of moisture in the environment are also important but are not separately expressed here. Following the notation of Weibull, the probability of failure s in glass may be expressed as

*Unpublished data.

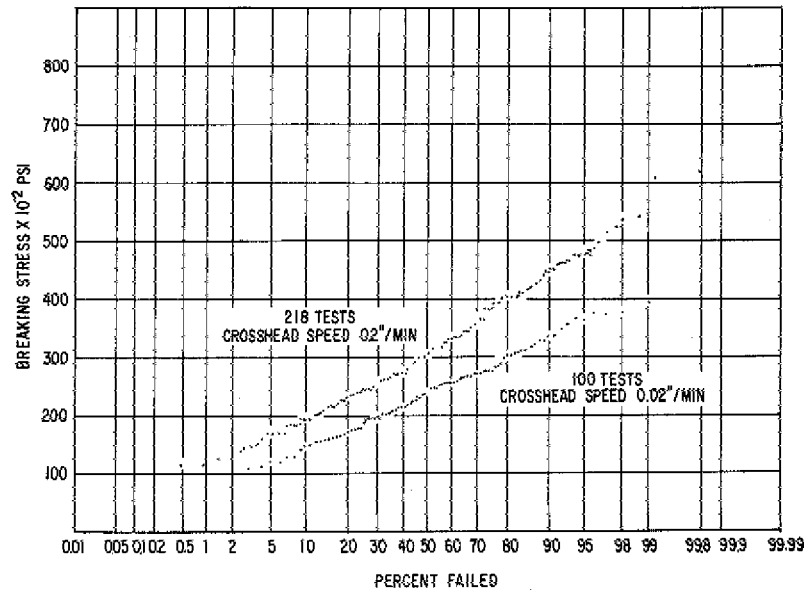


Fig. 1 - Applied stress vs probability of failure under rising load for two rates of crosshead motion. The specimens were lantern slides between concentric rings.

$$S = 1 - \exp - \int_0^A \left(\frac{\sigma}{\sigma_0} \right)^m \frac{dA}{A_0} \quad (1)$$

where A_0 is a small unit of area. The exponent is dimensionless. The integration is over that part of the area which is in tension. It is assumed that all effective flaws are on the surface and that σ_u , the lower limiting strength, is zero.

If the stress σ is constant over the area and A_0 is taken as unity,

$$S = 1 - \exp - \left(\frac{\sigma}{\sigma_0} \right)^m \frac{A}{1} \quad (2)$$

Using natural logarithms yields

$$\log \log \frac{1}{1-S} = m \log \sigma - m \log \sigma_0 + \log A \quad (3)$$

The constant σ_0 is evaluated by setting $S \approx 0.633$ or $\log 1/(1-S) = 1$ and $\log \log 1/(1-S) = 0$. Then

$$\sigma_0 = \sigma^* \left(\frac{A}{A_0} \right)^{1/m} \quad (4)$$

where σ^* is the stress corresponding to $S \approx 0.633$, and m is the Weibull coefficient. The constant σ_0 is a characteristic for the glass surface and is independent of size.

In making concentric-ring and other tests on glass plates, the values of σ_0 and of m are not expected to be representative of the corresponding coefficients for the internal bubbles. Higher values are to be expected for both in the bubble. For purposes of predictions based on tests of exposed surfaces not prestressed in any way, it is necessary to make a correction such that an artificially high strength is assigned to the test piece so that it represents the quality of the bubble surface. If the values of m and σ_0 are upgraded and the probability of failure is left unchanged, then for the test specimens one may write for any given probability of failure

$$\left(\frac{\sigma_1}{\sigma_{01}}\right)^{m_1} = \left(\frac{\sigma_2}{\sigma_{02}}\right)^{m_2}, \quad (5)$$

where σ_2 is the calculated strength of the test piece if m_2 and σ_{02} are the coefficients instead of the actual m_1 and σ_{01} . It follows that

$$\sigma_2 = \sigma_{02} \left(\frac{\sigma_1}{\sigma_{01}}\right)^{m_1/m_2}. \quad (6)$$

The values of σ_{01} and σ_{02} are independent and must be known or inferred from independent experiments. Sanford (4) has determined σ_{01} and σ_{02} representing as-received soda lime glass plates and plates etched by hydrofluoric acid. The area under uniform biaxial tensile stress was 1 sq in., and the values of σ_0 were

$$\sigma_{01} = 40,000 \text{ psi, untreated,}$$

$$\sigma_{02} = 250,000 \text{ psi, etched,}$$

and represented a separated distribution.

Representative values of m determined by Sanford were approximately

$$m_1 = 1.9 \text{ for as-received glass}$$

$$m_2 = 3.6 \text{ for the glass after etching.}$$

Both the values of m were lower than those found by Schmitz for carefully handled glass fibers (5). Schmitz-tested glass fibers received from the bushing and wound on a holder so that no contact of glass to glass is permitted have exhibited m values ranging up to 100. It was noted in that study that no single m value could be selected as representative. A simple way of determining m for fibers is by studying the effect of length on strength. Otto (6) provided the size-effect data shown in Fig. 6 of Ref. 5, from which one may deduce $m = 8.6$ for pristine E-glass fibers.

The Weibull coefficient m is an approximate measure of the standard deviation as shown by Irwin (7),

$$\eta = \frac{\sqrt{1.5}}{m}, \quad (7)$$

where η is the relative standard deviation from the mean strength.

THE SIZE EFFECT

When m and σ_0 are constants independent of size, it follows from Eq. (1) that for an equal probability of failure,

$$\left(\frac{\sigma}{\sigma_0}\right)^m A = \text{constant}$$

and

$$\frac{d \log \sigma}{d \log A} = \frac{-1}{m},$$

also, for sizes 1 and 2, the ratio of strengths is

$$\frac{\sigma_1}{\sigma_2} = \left(\frac{A_2}{A_1}\right)^{1/m} \quad (9)$$

for any given probability of failure.

If the m and σ_0 values are different between the test specimen and the object for which a prediction is made, Eq. (6) must be employed, and also an effective size or area must be used if the stress distribution is not uniform.

The effective area of an object is given by

$$A_{eff} = \left(\frac{1}{\sigma_{max}}\right)^m \int^A \sigma^m dA. \quad (10)$$

The integration is over that part of the area on which a tensile stress exists. The effective area is also defined as the area of another specimen having equal probability of failure under a uniformly distributed stress $\sigma = \sigma_{max}$, where σ_{max} is as given in Eq. (10).

From simple beam theory, the effective area of a rectangular beam in three-point loading is accordingly

$$A_{eff} = \frac{L}{m+1} \left(b + \frac{D}{m+1}\right), \quad (11)$$

where L is the span and b and D are the width and depth, respectively.

For a circular cross section of radius r the effective area of a beam in three-point loading is

$$A_{eff} = \frac{2rL [2 \times 4 \times 6 \times \dots, (m-1)]}{(1 \times 3 \times 5 \times \dots, m)} \quad \text{if } m \text{ is an odd integer} \quad (12)$$

and

$$A_{eff} = \frac{\pi rL [1 \times 3 \times 5 \dots, (m-1)]}{(m+1) (2 \times 4 \times 6 \dots, m)} \quad \text{if } m \text{ is an even integer.} \quad (13)$$

In predicting the strength of an object based on tests of specimens of different sizes, it is not necessary to use effective sizes if the specimens are geometrically similar and are similarly loaded. In that case the ratio of gross areas is the same as the ratio of effective areas. When predictions are made based on comparisons between geometrically dissimilar specimens, effective areas must be used in Eq. (9).

EFFECTIVE AREAS OF ELLIPSOIDAL CAVITIES UNDER COMPRESSIVE LOADING — SPECIAL CASES

Sample problems representing worst cases are presented in this section for purposes of demonstrating the method of calculating and for making quantitative strength predictions based on assumed values of σ_0 and m .

Uniaxial Compression, Spherical Cavity

For uniaxial compression it was shown in Ref. 3 that a spherical cavity was the worst-case shape for prolate ellipsoids aligned with the prolate axis parallel with the applied stress. The tensile stress on the surface of the cavity can be represented to a good approximation by

$$\sigma = \sigma_{max} \cos 2\theta, \quad (14)$$

where θ is the angle between the pole of the sphere and the element of area in the spherical cap. When $\theta = 0$, $\sigma = \sigma_{max}$ and when $\theta = \pi/4$, $\sigma = 0$. The element of area dA is $R^2 \sin \theta d\theta d\phi$.

The effective area of the spherical bubble is then

$$A_{eff} = 8 \left(\frac{1}{\sigma_{max}} \right)^{1/m} \int_0^{\pi/2} \int_0^{\pi/4} \sigma_{max}^m (\cos 2\theta)^m R^2 \sin \theta d\theta d\phi$$

or

(15)

$$A_{eff} = 4\pi R^2 \int_0^{\pi/4} (\cos 2\theta)^m \sin \theta d\theta.$$

A plot of $A_{eff}/(4\pi R^2)$ vs m is shown in Fig. 2. In Ref. 3 the spherical cavity was shown to develop $\sigma_{max} = |\sigma|$ applied for Poisson's ratio $\nu = 0.45$ and for an applied uniaxial compressive stress. For $\nu = 0.25$, $\sigma_{max} = 0.58 \sigma$ applied. These factors will be taken into account later in estimating the compressive strength of a block of glass for fracture initiating at an internal bubble.

Needle-Shaped Cavity, Parallel with Shell Axis, in a Cylindrical Shell Under Hydrostatic Pressure

In this case of a needle-shaped cavity in a cylindrical shell under hydrostatic pressure, the prolate axis is parallel with the cylindrical shell axis.

In accordance with Ref. 3, a good approximation for the tensile stress on the cavity surface is

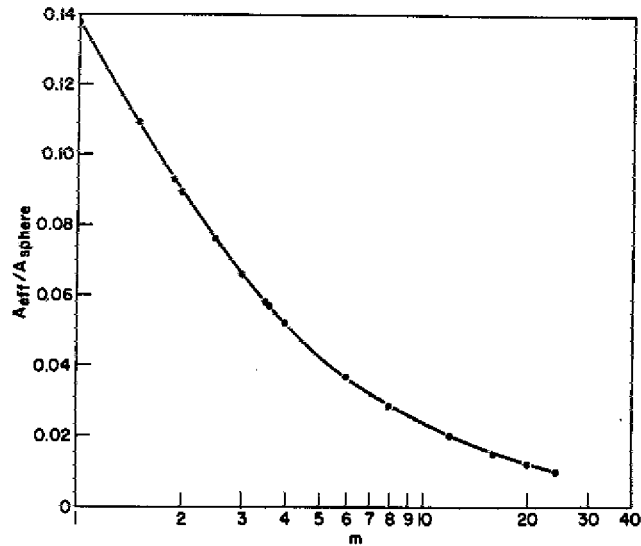


Fig. 2 - The ratio of effective area to total area for a spherical cavity in an infinite medium under a uniaxial, compressive stress. This is a function of the Weibull coefficient m .

$$\sigma = \sigma_{max} \cos 2\theta. \quad (16)$$

The element of area is

$$dA = R d\theta dL,$$

where dL is an increment of length of the cavity and R is the minor semiaxis. The effective area is

$$A_{eff} = 4 \left(\frac{1}{\sigma_{max}} \right)^m \int_0^{\pi/4} \int_0^L \sigma^m R d\theta dL$$

or

$$A_{eff} = 4RL \int_0^{\pi/4} (2 \cos^2 \theta - 1)^m d\theta. \quad (17)$$

A plot of $A_{eff}/(2\pi RL)$ vs m is shown in Fig. 3.

The needle-shaped cavity was selected here as being the prolate ellipsoid shape which would see the highest tensile stress for the given orientation. For the case selected, the value of σ_{max} is the same as the magnitude of the compressive membrane stress for all values of Poisson's ratio. If shapes approaching the spherical had been selected, the values of σ_{max} would have been dependent on Poisson's ratio as shown in Ref. 3. The tensile stresses are not in a perfect biaxial relationship, as they are for the preceding case.

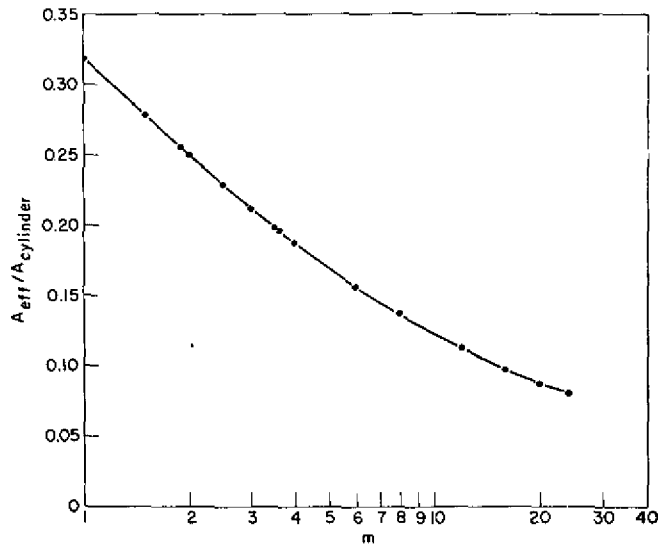


Fig. 3 - The ratio of effective area to total area for a needle-shaped cavity in the wall of a cylindrical shell under hydrostatic pressure. The prolate axis is parallel with the cylinder axis. A further correction is to be made to account for the uniaxial stress when a prediction is to be made based on a biaxial test.

To make the adjustment so as to calculate the effective area for uniaxial stress, we assume that for every direction there is the same distribution of flaw density and severity and that the stress σ is normal to the same number of flaws in each category of size for the 1:1 stress situation. For uniaxial stress let σ_r = resolved normal stress for any flaw; then

$$\sigma_r = \sigma_{max} \cos \theta.$$

Assume that the flawed area in question is made up of circles which are nested to fill all of the area and that each is representative of the whole. For any circle σ_{max} is unidirectional. The area element is $\rho^2 d\theta/2$.

By definition

$$A_{eff} = \left(\frac{1}{\sigma_{max}} \right)^m \int^A (\sigma_r)^m dA$$

or

$$A_{eff} = \left(\frac{1}{\sigma_{max}} \right)^m \int_0^{\pi/2} \sigma_{max}^m (\cos \theta)^m \rho^2 \frac{d\theta}{2}$$

for any circle.

In the original Weibull concept, only uniaxial stress was considered or at least specified; however, we now find it convenient to have areal comparisons on the concentric-ring test. In Eqs. (11), (12), and (13) the calculation of effective area has used only one component of stress and assumed that the greatest principal tensile stress was the only one to be included. For a concentric-ring test $\sigma = \sigma_{max}$ for all values of θ . So by definition, $A_{eff} = A_{total}$ for the concentric-ring test and

$$f = \frac{2}{\pi} \int_0^{\pi/2} (\cos \theta)^m d\theta, \quad (18)$$

where f is the ratio of the effective area for uniaxial stress to the effective area for biaxial stress on a circle of any radius. A plot of Eq. (18) is shown in Fig. 4.

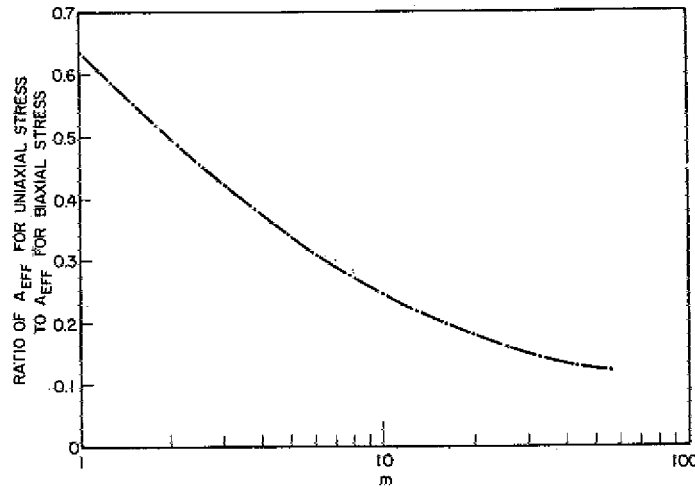


Fig. 4 - The ratio of the effective area under uniaxial stress to the effective area for a biaxial tensile stress as a function of the Weibull coefficient m

An arbitrary selection of $L = 20R$ was made for purposes of illustration in the figures for needle-shaped cavities. However, for other L values the predicted strengths σ_{b2} for $L = L_2$ would be given in terms of σ_{b1} already computed as

$$\sigma_{b2} = \sigma_{b1} \left(\frac{L_1}{L_2} \right)^{1/m_2} \quad (19)$$

This assumes that R is constant and L varies.

For $m_2 = 12$ the effect of doubling the length of a cavity would be to reduce its predicted strength by 6 percent.

Needle-Shaped Cavity Parallel with a Spherical Shell Wall Under Hydrostatic Pressure

The prolate ellipsoid seeing the highest tensile stress is the needle-shaped cavity. The surface stress is equal in magnitude to the compressive membrane stress, whereas a spherical cavity would experience a tensile stress about half as large.

As a good approximation of the surface tensile stresses in the needle-shaped cavity in the wall of a hollow sphere, we write

$$\sigma = \sigma_{max} \cos 3\theta. \quad (20)$$

The element of area is

$$dA = R \, d\theta \, dL,$$

and the effective area for hydrostatic compressive loading is

$$A_{eff} = 4RL \int_0^{\pi/6} (\cos 3\theta)^m \, d\theta$$

or

(21)

$$A_{eff} = 4RL \int_0^{\pi/6} (4 \cos^3 \theta - 3 \cos \theta)^m \, d\theta.$$

The ratio of the effective area to the total area of a long cylinder is plotted in Fig. 5 as a function of the Weibull coefficient m . Here as in the preceding case the tensile stresses are essentially uniaxial.

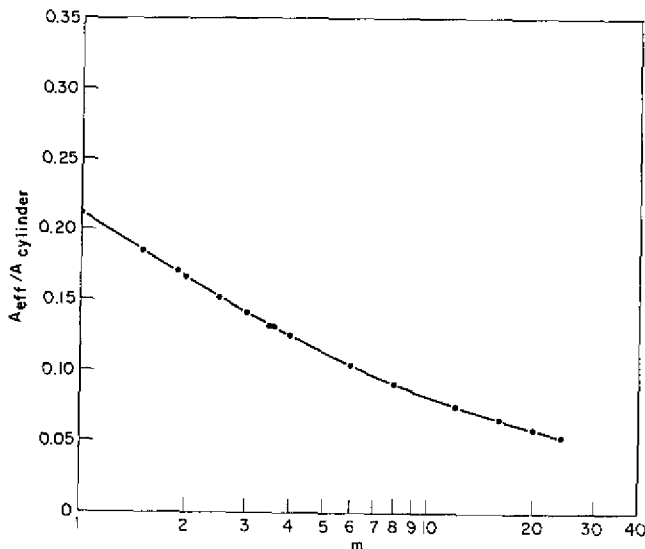


Fig. 5 - The ratio of effective area to total area for a needle-shaped cavity in a spherical shell. The prolate axis is parallel with the shell wall. A further correction is to be made to account for uniaxial stress when a prediction is to be made based on a biaxial test.

Spherical Cavity in a Spherical Shell Under Hydrostatic Pressure

The magnitude of the maximum tensile stress on the surface of the cavity is about 55 percent of the membrane compressive stress in the shell, instead of being 100 percent as for the needle-shaped cavity. This case is included here because it is likely to occur. The maximum tensile stress generated is nearly uniaxial, is normal to the surface of the spherical shell, and is constant for all positions in the shell. The tendency is to cause splitting, which resembles delamination or spallation of the shell. Figure 6 shows the effective area of the spherical cavity as a function of the Weibull coefficient m for this case.

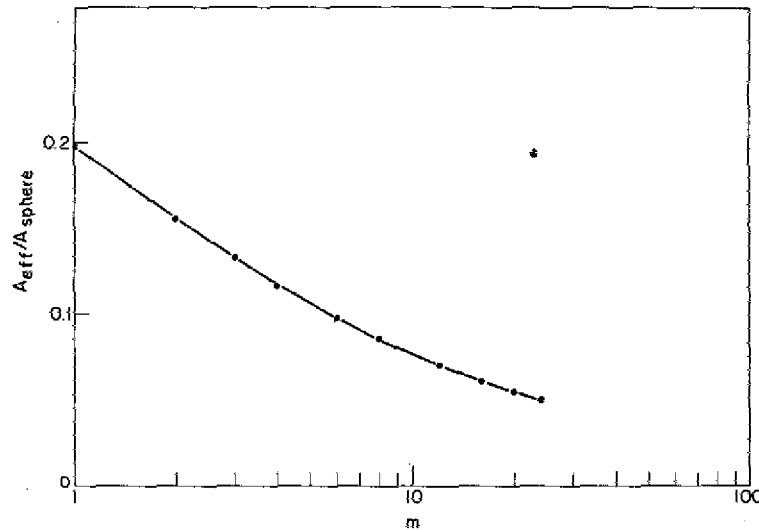


Fig. 6 - The ratio of effective area to total area of a spherical cavity embedded in a spherical shell. A further correction is to be made to account for the uniaxial stress when a prediction is to be based on a biaxial test.

PREDICTED FRACTURE STRENGTH OF INTERNAL CAVITIES

The effects of size on strength and the estimated tensile stresses in cavities are now combined in order to predict the breaking strength for fractures spreading out from the walls of the cavities. The mathematical model employed here predicts bubble wall strength in terms of the strength of plates tested between concentric rings. It is assumed that σ_0 and m are different for the bubble and for the test piece.

Let σ_2 be the idealized strength of the plate whose actual strength is σ_1 . The idealized strength representing bubble-surface quality was given in Eq. (6). It is assumed that σ_{02} and m_2 are Weibull constants representative of the bubble surface as well as the idealized test specimen and that σ_{01} and m_1 are representative of the actual test plates. Let σ_b be the predicted strength of the bubble at an arbitrarily selected probability of failure.

If we refer to Eq. (2) and set the probability of failure at some arbitrary value, then

$$\left(\frac{\sigma_1}{\sigma_{01}}\right)^{m_1} A_{1 \text{ eff}} = \left(\frac{\sigma_2}{\sigma_{02}}\right)^{m_2} A_{2 \text{ eff}} = \left(\frac{\sigma_b}{\sigma_{02}}\right)^{m_2} A_{b \text{ eff}}. \quad (22)$$

where $A_{b\ eff}$ is the effective area of the bubble. Since the inner circle of the test piece is under uniform stress, both the effective areas $A_{1\ eff}$ and $A_{2\ eff}$ are the actual area A_1 of the inner circle of the test piece. Then

$$\frac{\sigma_b}{\sigma_2} = \left(\frac{A_1}{A_{b\ eff}} \right)^{1/m_2} \tag{23}$$

Substituting from Eq. (6), we have the predicted bubble strength at the selected equal probability of failure as

$$\sigma_b = \frac{\sigma_{02}}{\sigma_{01}^{m_1/m_2}} \sigma_1^{m_1/m_2} \left(\frac{A_1}{A_{b\ eff}} \right)^{1/m_2} \tag{24}$$

To make numerical estimates of the bubble strength σ_b , we must specify σ_{02} and m_2 . In lieu of such direct experimental knowledge and for purposes of illustration, we now assume that the bubble is represented by $\sigma_{02} = 250,000$ psi as it was for the Sanford tests of etched plates. In the Sanford tests the effective area was 1 in.² and in accordance with Eq. (4), $\sigma^* = \sigma_0$ etched.

In using the mathematical model given in Eq. (24), we further choose $m_1 = 1.9$ for the test specimens as found by Sanford.

Solutions of Eq. (24) are shown graphically in a series of figures according to bubble shape and shell type.

Spherical Cavity Under Applied Uniaxial Compressive Stress

Selected values of predicted strength for various cavity sizes and probabilities of fracture are shown in Figs. 7 and 8. Figure 7 shows the maximum tensile stress in the

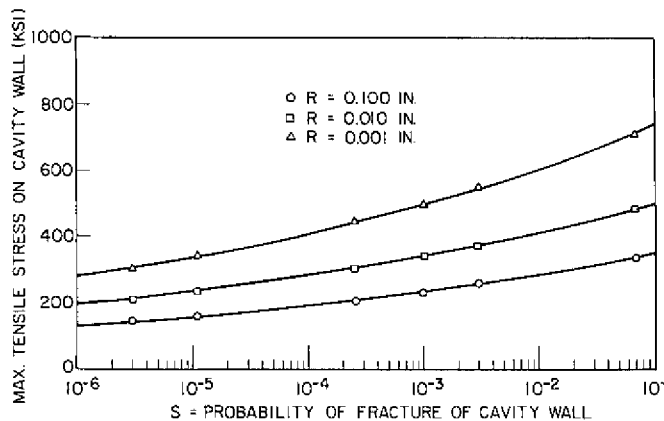


Fig. 7 - Predicted strength of a spherical cavity in a field of uniaxial compressive stress as a function of probability of failure. For a Poisson ratio of 0.25, the applied compressive stress is 1.82 times the maximum tensile stress in the cavity. R is the minor semiaxis of the cavity.

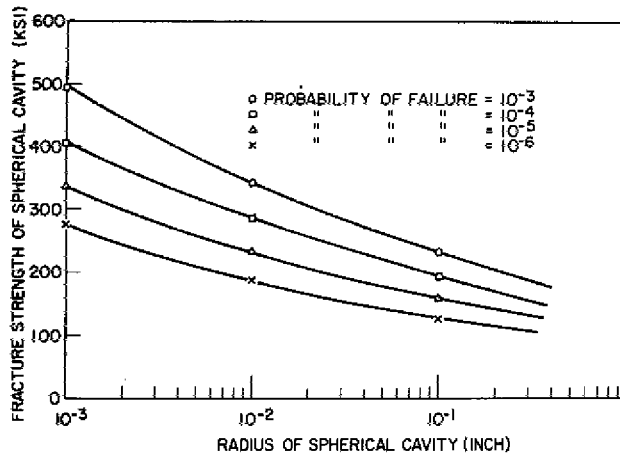


Fig. 8 - The effect of spherical cavity size on predicted strength for four selected levels of probability of failure predicted under applied uniaxial stress. All strengths are proportional to the Weibull constant $\sigma_{0.2}$, chosen here as 250 ksi, as obtained from tests on soda lime glass etched by hydrofluoric acid.

cavity plotted against the probability of fracture for three cavity sizes with a probability of $S = 1 \times 10^{-6}$, the lowest risk value shown, and for $m = 12$ only. For risk values smaller than 10^{-6} the strengths are only slightly lower. The maximum tension on the cavity wall is numerically equal to the applied compressive stress for Poisson's ratio $\nu = 0.45$, but for glass, when $\nu = 0.25$, the stress on the bubble σ_b is only 55 percent of the applied compressive stress. For a cavity having a radius of 0.1 in. or less, the predicted gross stress in the glass at failure is then at least 245 ksi. For an expected shell membrane stress, a safety factor on stress is accordingly 2.45 with no allowance for long-term degradation by static fatigue of the cavity wall. Figure 8 shows more directly the effect of cavity size on strength. All strengths shown are directly proportional to the Weibull constant σ_0 , herein specified as $\sigma_{0.2} = 250$ ksi, which is assumed as characteristic of the cavity wall at $S = 0.633$.

Needle-Shaped Cavity in a Cylindrical Shell Under Hydrostatic Compression

The prolate axis is parallel with the axis of the cylinder in the case of the needle-shaped cavity in a cylindrical shell considered here.

The needle-shaped cavity experiences the highest tensile stress of any prolate ellipsoid. The maximum stress is uniaxial and directed normal to the surface of the shell. The tendency is to produce spalling or what would appear to be delamination. The stress is independent of Poisson's ratio in this case. In calculating effective areas, Eq. (17) and Fig. 3 are used. In addition, a further multiplying factor given by Eq. (18) and shown in Fig. 4 is applied to allow for uniaxial stress in the cavity. This factor is included because the strength predictions are to be made on the basis of biaxial stress tests of plates between concentric rings. An equivalent statement is that the effective area of the test piece under biaxial stress is greater than its actual area for purposes of predicting the strength of another area under uniaxial stress. The effective area of the test piece for the purpose is then $A_{eff} = A/f$, where

$$f = \frac{2}{\pi} \int_0^{\pi/2} \cos^m \theta d\theta.$$

The predicted cavity strength is shown in Fig. 9 as a function of the probability of failure, and in Fig. 10 the effect of cavity size on fracture strength is shown for four

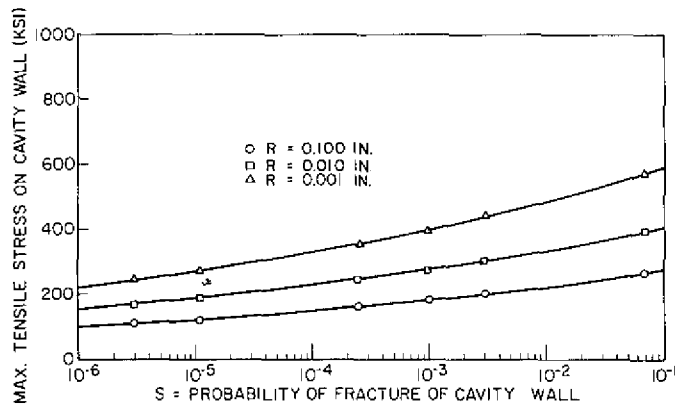


Fig. 9 - Predicted strength of a needle-shaped cavity in a cylindrical shell as a function of the probability of failure. The maximum tensile stress in the cavity wall is equal in magnitude to the applied hoop stress in the cylinder. The prolate axis is parallel to the cylinder axis.

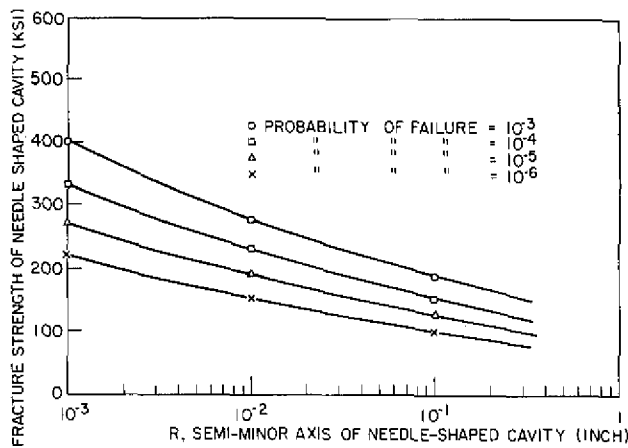


Fig. 10 - The effect of size of a needle-shaped cavity on the predicted strength for four selected probabilities of failure in a cylindrical shell under hydrostatic compression

selected probabilities of failure. For the needle-shaped cavity, the predicted strength is independent of Poisson's ratio and is numerically equal to the applied compressive hoop stress in the cylinder for the cavity orientation being considered.

Needle-Shaped Cavity in a Spherical Shell

The predicted cavity strength is shown in Fig. 11 as a function of probability of failure, and the effect of cavity size on strength is shown in Fig. 12. The maximum tensile stress in the cavity is independent of Poisson's ratio and is equal in magnitude to the compressive membrane stress in the shell. The needle shape is the worst case.

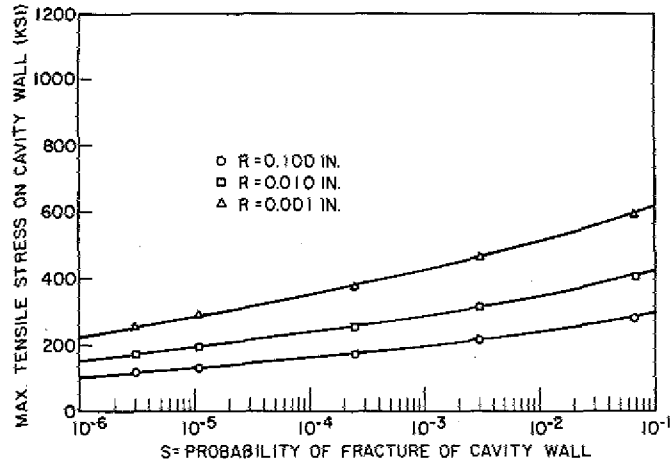


Fig. 11 - Predicted strength of a needle-shaped cavity in a spherical shell as a function of probability of failure. The applied membrane stress is equal to the predicted strength in magnitude and is independent of Poisson's ratio.

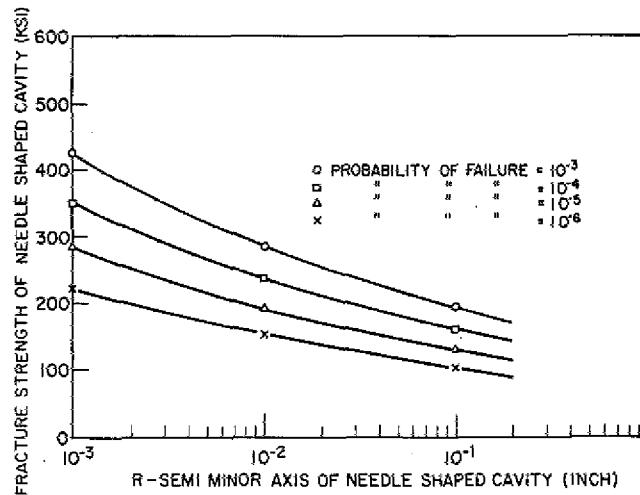


Fig. 12 - The effect of needle-shaped cavity size on strength for four selected probabilities of failure in a spherical shell

Spherical Cavity in a Spherical Shell

The predicted cavity strength is shown in Fig. 13 as a function of the probability of failure and in Fig. 14 as a function of cavity size for four selected probabilities of failure. The ratio of the stress in the cavity to the applied membrane stress is somewhat dependent on Poisson's ratio for the spherical cavity. In this case the maximum tensile stress is directed in such a way as to tend to produce a splitting that resembles delamination in the shell. It is of constant magnitude around an equatorial belt of the cavity. The ratio of maximum tensile stress $\sigma_{y \max}$ to applied membrane stress P was computed to be

$$\sigma_{y \max} = -\frac{3P}{7 - 5\nu}, \quad (25)$$

where ν is Poisson's ratio. For $\nu = 0.23$, $\sigma_{y \max} = -0.513P$. In other words the membrane stress necessary to cause fracture failure in the bubble is 1.95 times the bubble strengths indicated in Figs. 13 and 14 for glass.

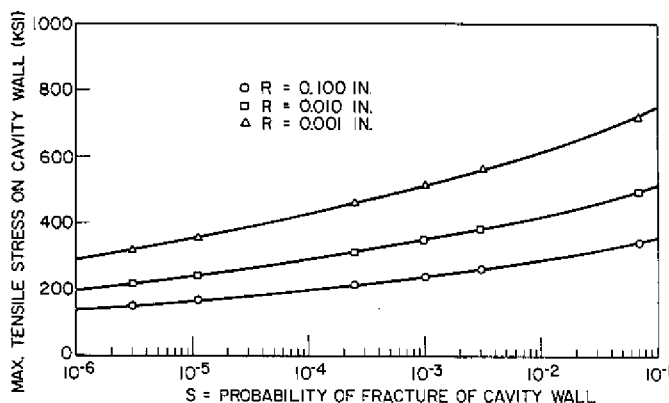


Fig. 13 - Predicted strength of a spherical cavity in a spherical shell as a function of the probability of failure. The applied membrane stress is 1.95 times the maximum tensile stress in the bubble for a Poisson ratio of 0.23.

CONCLUSIONS

1. All of the foregoing predictions of strength are intended as illustrative examples dependent on the mathematical model as described. Selected but hopefully reasonable values of the Weibull m and σ_0 coefficients were used in order to arrive at numerical predictions.

2. The predicted strengths are directly proportional to σ_0 set here at 250 ksi. It would be well to establish this coefficient for surfaces more truly representative of internal cavities. This would require several hundred tests. Ernsberger (8) recently measured the tensile strengths of internal cavities and obtained values as high as 1600 ksi, but statistical distributions were not included.

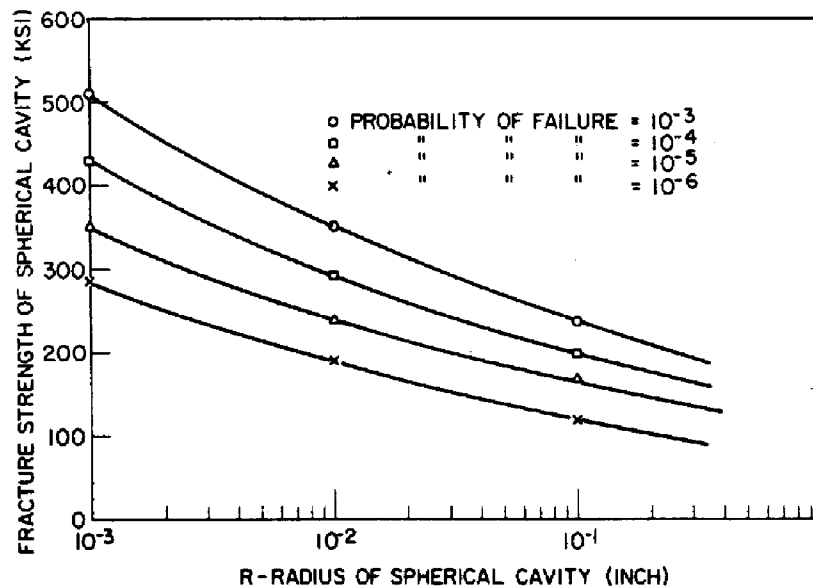


Fig. 14 - The effect of size on the strength of a spherical cavity in a spherical shell for four selected probabilities of failure

3. The predicted strengths shown in the figures are for the maximum stresses on the walls of the cavities. In some cases these are equal in magnitude to the applied compressive stress in the shell and in other cases the tolerable applied membrane stress would be nearly twice as much as noted in the text.

4. For manned vehicles extreme reliability is required so that the probability of failure should be less than 10^{-5} or perhaps 10^{-6} . Indicated tensile strengths of cavities for this low probability of failure are all above 100 ksi for bubbles of 0.1-in. radius or less.

5. All predictions were based on the assumption of the Weibull coefficient $m = 12$. Although $m = 12$ has in the past been found representative of pristine glass filaments, we do not have a direct determination for bubbles. The results are not highly sensitive to m in the range of $m = 12$ to 20, as is illustrated in Fig. 15. Therein the predicted strengths of bubbles are plotted vs m for three different bubble sizes embedded in a spherical shell.

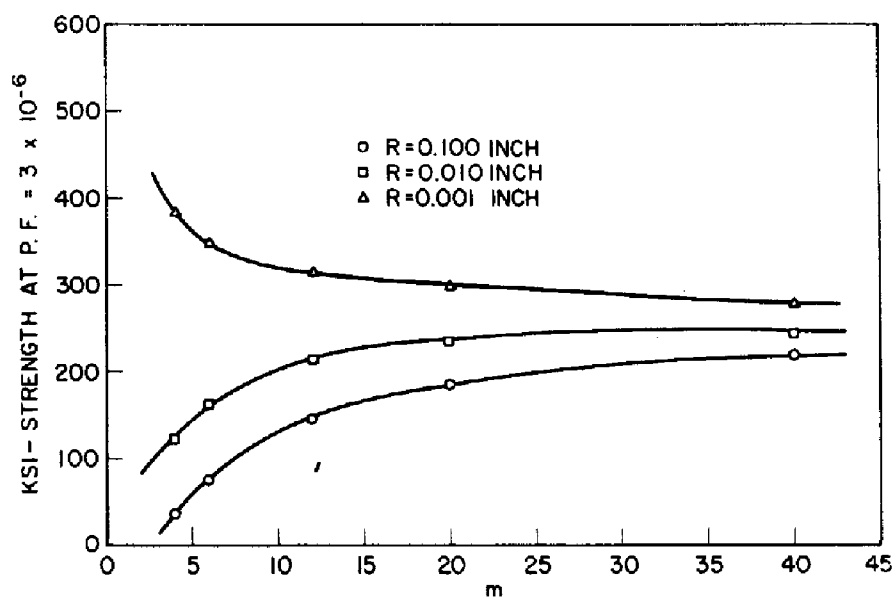


Fig. 15 - The effect of the Weibull m coefficient on predicted strength for three sizes of bubbles and for a selected probability of failure of 3×10^{-6}

6. In view of the foregoing calculations and considerations, it seems reasonable to conclude that for single spherical cavities of 0.1 in. or less in radius and for single needle-shaped cavities whose cross-sectional radius is 0.1 in. or less the probability of failure is less than 10^{-6} for imposed compressive membrane stresses of 100 ksi or less. In the course of hydrotesting glass spheres, fracturing initiating at single cavities has been rare but spallation starting from clusters of cavities has been frequent.

7. For clusters of cavities in which a small satellite bubble is near a larger bubble, a superimposed tensile stress multiplier of about 2 would be imposed. This indicates that for a 10^{-6} probability of failure the membrane stress should be kept at 50 ksi or less. Stresses and predicted strengths for clusters of cavities remain to be calculated.

8. The effects of a long time under load have been neglected in this report for the reason that environmental attack, as by moisture in bubbles, is expected to be nonexistent. If moisture present in the glass can migrate to the cavities, then this assumption may not be valid. Long-time compressive loading tests on glasses containing bubbles are to be desired.

9. It should be carefully noted that suitable fracture mechanics formulas for the cases discussed are not available (9). In each of the cases the effective driving force \mathcal{G} or the stress-intensity factor would at first increase with crack depth as a crack progresses into the material starting at the cavity wall. As the crack deepens, however, the tensile stress field would decrease and a limit on the extension of the crack should be expected. A prediction of how far a crack would propagate before arrest has not been made.

REFERENCES

1. Perry, H.A., and others, "Massive Glass Hull for Deep Submergence Vehicle," Naval Ordnance Laboratory Technical Program Plan for the Naval Ship Systems Command under S4728-005, Task 12327 Jan. 1968
2. Golightly, J.S., "Fabrication of 56-inch Diameter Glass Hemispheres for Underwater Capsules," published in "The Decade Ahead 1970-1980," a symposium sponsored by the Marine Technology Soc., Miami, June 1969
3. Mulville, D.R., and Kies, J.A., "Tensile Stresses on the Surface of an Ellipsoidal Cavity in Compressive Loading Situations," NRL Report 6210, Mar. 1965
4. Sanford, R.J., and Withrow, S.P., "Strength Distribution of Etched Glass," NRL Report of Progress Sept. 1967, pp. 33-35
5. Schmitz, G.K., and Metcalfe, A.G., "Exploration and Evaluation of New Glasses in Fiber Form," Final Summary Report, Contract NONR 3654(00)(x) to the Solar Div., Int'l. Harvester Co., San Diego, Calif., May 20, 1965
6. Otto, W.H., Private communication, Narmco Research and Development Co., San Diego, Calif. at the time; now with Ryan Corp., San Diego, Calif.
7. Irwin, G.R., "The Effect of Size Upon Fracturing," Symposium on Effect of Temperature on the Brittle Behavior of Metals with Particular Reference to Low Temperatures," Am. Soc. Testing Materials Spec. Tech. Pub. 158:176 (1954)
8. Ernsberger, F.M., "Tensile and Compressive Strength of Pristine Glasses," Am. Ceramic Soc. Paper 45-G-69, 71st Annual Meeting, April 1969, Washington, D.C. (to be published)
9. Kies, J.A., "Fracture in Materials under Compression Loading," published in "The Decade Ahead 1970-1980," a symposium sponsored by the Marine Technology Soc., Miami, June 1969